HHS Public Access

Author manuscript

J Mol Cell Cardiol. Author manuscript; available in PMC 2017 October 01.

Published in final edited form as:

J Mol Cell Cardiol. 2016 October ; 99: 87–99. doi:10.1016/j.yjmcc.2016.08.019.

Deletion of Calponin 2 in Macrophages Alters Cytoskeleton-based Functions and Attenuates the Development of Atherosclerosis

Rong Liu and **J.-P. Jin***

Department of Physiology, Wayne State University School of Medicine, Detroit, MI, USA

Abstract

Arterial atherosclerosis is an inflammatory disease. Macrophages play a major role in the pathogenesis and progression of atherosclerotic lesions. Modulation of macrophage function is a therapeutic target for the treatment of atherosclerosis. Calponin is an actin-filament-associated regulatory protein that inhibits the activity of mosin-ATPase and dynamics of the actin cytoskeleton. Encoded by the gene *Cnn2*, calponin isoform 2 is expressed at significant levels in macrophages. Deletion of calponin 2 increases macrophage migration and phagocytosis. In the present study, we investigated the effect of deletion of calponin 2 in macrophages on the pathogenesis and development of atherosclerosis. The results showed that macrophages isolated from *Cnn2* knockout mice ingested a similar level of acetylated low-density lipoprotein (LDL) to that of wild type (WT) macrophages but the resulting foam cells had significantly less hindered velocity of migration. Systemic or myeloid cell-specific *Cnn2* knockouts effectively attenuated the development of arterial atherosclerosis lesions with less macrophage infiltration in apolipoprotein E knockout mice. Consistently, calponin 2-null macrophages produced less pro-inflammatory cytokines than that of WT macrophages, and the up-regulation of pro-inflammatory cytokines in foam cells was also attenuated by the deletion of calponin 2. Calponin 2-null macrophages and foam cells have significantly weakened cell adhesion, indicating a role of cytoskeleton regulation in macrophage functions and inflammatory responses, and a novel therapeutic target for the treatment of arterial atherosclerosis.

Graphical abstract

*Send correspondence to: Dr. J.-P. Jin, Department of Physiology, Wayne State University School of Medicine, 540 E. Canfield, Detroit, MI 48201, USA. jjin@med.wayne.edu.

Disclosure

None.

Deletion of calponin 2 in macrophages attenuates the atherosclerotic lesions in *ApoE*$^{-/-}$ mice

Keywords

Calponin; macrophage; atherosclerosis; cell motility; cell adhesion; ApoE knockout mouse

1. Introduction

Atherosclerosis is the primary cause of ischemic heart disease and stroke. In the past two decades, studies have established that atherosclerosis is an inflammatory disease (Ross, 1999) (Libby, 2012) (Nahrendorf and Swirski, 2015). Increasing levels of circulating low-density lipoprotein (LDL)-cholesterol and the subsequent intramural accumulation of oxidized LDL trigger the recruitment and retention of monocytes to generate subendothelial lesions in arterial wall (Lusis, 2000). In the intima of vessel wall, monocytes differentiate into macrophages to scavenge lipoprotein particles and become foam cells, which is a landmark of atherosclerosis (Lusis, 2000). Macrophages and the lipid ingestion-generated foam cells play active roles in mediating the ensuing inflammatory response and prognosis of atherosclerosis plaques (Chinetti-Gbaguidi et al., 2015). Therefore, the regulation of macrophage activation and function has become a focus of the exploration of new therapeutic approaches for arterial atherosclerosis.

To date, the regulation of macrophage function in atherosclerosis and other inflammatory diseases has been investigated mainly in the context of ligand-receptor recognitions and the effects on cell signaling. While the motility and substrate adhesion of macrophages play essential roles in the development and resolution of inflammation (Patel et al., 2012) (Sosale et al., 2015), very little is known about how the regulation and mechanisms by which these cytoskeleton mechanical tension-based functions determine the development and prognosis of atherosclerosis.

Calponin is a family of actin filament-associated regulatory proteins of 34–37 kDa (292–330 amino acids) in size found in smooth muscle (Takahashi et al., 1986) and many non-muscle cell types (Hossain et al., 2005) (Hossain et al., 2006). Through high affinity binding to F-actin, calponin inhibits the actin-activated myosin MgATPase (Winder and Walsh, 1990) (Abe et al., 1990) (Winder et al., 1993) and motor activity (Shirinsky et al., 1992) (Haeberle, 1994). Three isoforms of calponin have been found in vertebrate species (Liu and Jin, 2016): A basic calponin (calponin 1, isoelectric point (pI) = 9.4) expresses specifically in mature smooth muscle cells and functions in regulating smooth muscle contractility (Walsh, 1991; Nigam et al., 1998; Hossain et al., 2003; Jin et al., 2008; Wu and Jin, 2008). An acidic calponin (calponin 3, pI = 5.2) is found in brain (Trabelsi-Terzidis et al., 1995), embryonic trophoblasts (Shibukawa et al., 2010) and myoblasts (Shibukawa et al., 2013) to participate in cell fusion during embryonic development and myogenesis. Calponin 2 is an isoform with neutral overall charge (pI=7.5) and presents in a broad range of tissue and cell types, including smooth muscle cells (Hossain et al., 2003), endothelial cells (Tang et al., 2006), epithelial cells, fibroblasts (Hossain et al., 2005; Hossain et al., 2006), and myeloid leukocytes (Huang et al., 2008). Via decreasing the dynamics and stabilizing the actin

cytoskeleton, calponin 2 regulates many actin-cytoskeleton-based cellular functions such as increasing substrate adhesion and inhibiting migration and cytokinesis.

Calponin 2 is expressed at significant levels in macrophages. A previous study in our laboratory has demonstrated that calponin 2 regulates migration and phagocytosis of macrophages. Peritoneal macrophages isolated from *Cnn2* gene knockout (KO) mice exhibited a faster rate of migration and enhanced phagocytosis than that of wild type (WT) control cells, indicating a regulatory role of calponin 2 in the fundamental function of macrophages (Huang et al., 2008). Following this novel discovery, the present study investigated the effect of deleting calponin 2 in macrophages on the pathogenesis and development of arterial atherosclerosis. Using cellular and *in vivo* mouse models, the experiments demonstrated that macrophages isolated from *Cnn2* KO mice ingest a similar level of LDL to that of WT macrophages but the resulting foam cells had less impairment in migration. Consistently, *Cnn2* KO in myeloid cells effectively attenuated the development of arterial atherosclerosis lesions in apolipoprotein E knockout mice. Supporting the identification of calponin 2 as a novel therapeutic target, calponin 2-null macrophages produced less pro-inflammatory cytokines than that of WT macrophages, and the up-regulation of pro-inflammatory cytokines in foam cells was also attenuated by the deletion of calponin 2. Calponin 2 null macrophages exhibit a weakened adhesion to substrate, linking a cytoskeleton regulation to macrophage activity and inflammatory response.

2. Materials and methods

2.1. Genetically modified mice

All animal studies were carried out under protocols approved by the Institutional Animal Care and Use Committee of Wayne State University.

The generation and initial characterization of *Cnn2*-floxed ($Cnn2^{f/f}$) mice and induction of systemic *Cnn2* KO have been described previously (Huang et al., 2008). The colony of $Cnn2^{-/-}$ mice has been backcrossed with wild type C57BL/6 mice for 9 or more generations, ensuring >99% of C57BL/6 genetic background. Myeloid cell-specific *Cnn2* KO mice ($Cnn2^{f/f}$,$lysM^{cre+}$) were generated by cross-breeding $Cnn2^{f/f}$ mice with $lysM^{cre+}$ mice, a transgenic line in C57BL/6 strain bearing a Cre recombinase gene driven by *lys*M promoter (Clausen et al., 1999) (Huang et al., 2010). The effectiveness of lysM-Cre induced targeting of *Cnn2* gene in myeloid cells was confirmed as shown in a recent study that calponin 2 protein was undetectable in macrophages but unaffected in the skin (a representative control tissue) of $Cnn2^{f/f}$,$lysM^{cre+}$ mice (Huang et al., 2016). Apolipoprotein E (*ApoE*) gene KO mice (Piedrahita et al., 1992) (C57BL/6 strain) were purchased from TACONIC. $ApoE^{-/-}$,$Cnn2^{-/-}$ double homozygotes and $ApoE^{-/-}$,$Cnn2^{f/f}$,$lysM^{cre+}$ triple transgenic mice were produced by crossing $ApoE^{-/-}$ with $Cnn2^{-/-}$ and $Cnn2^{f/f}$,$lysM^{cre}$ lines. Genotypes of these experimental mice were confirmed using PCR and verified post mortem using Western blot analysis.

2.2. Preparation and culture of mouse macrophages

Residential peritoneal macrophages were lavaged with pre-warmed RPMI 1640 medium from WT and *Cnn2*$^{-/-}$ mice. Elicited mouse peritoneal macrophages were obtained by injection of 2 mL of sterile 3% thioglycollate broth for 72 h prior to lavage. A fixed volume (8 mL) of medium was used for each animal so the total number of cells lavaged could be compared. The cells collected were cultured in RPMI-1640 medium containing 10% fetal bovine serum (FBS), 2 mM L-glutamine, 100 i.u./mL penicillin and 50 i.u./mL streptomycin at 37°C in 5% CO_2 unless specified.

2.3. Macrophage lipid engulfment

Residential peritoneal macrophages were isolated from WT and *Cnn2*$^{-/-}$ mice as above and seeded onto pre-cleaned coverslips in a 48-well culture plate in RPMI 1640 medium containing 10% FBS. Cells were allowed to adhere to the coverslips at 37°C overnight. Non-adherent cells were removed by gentle washing with pre-warmed RPMI 1640 medium. The adherent macrophages were processed for experiments as described (Zhang et al., 2008). To load the macrophages with lipid, the culture medium was switched to RPMI 1640 containing 10% FBS and 25 μg/mL acetylated LDL (BT-906, Alfa Aesar). The cells on coverslips were fixed at 4 hrs, 8 hrs and 24 hrs of lipid loading and the formation of lipid laden foam cells was examined by staining the intracellular lipid droplets with 60% Oil Red O (O0625, Sigma-Aldrich) in isopropanol at room temperature for 5 minutes. Cell nucleus was counter-stained with Mayer's hematoxylin (26043-06, Sigma-Aldrich) for 5 min. The stained coverslips were mounted on glass slides and photographed using a Zeiss Axiovert 100 microscope. The formation of foam cells was quantified in at least 10 representative view fields in different areas of each coverslip using ImageJ 64 software (NIH, Bethesda, MD). The assay was performed in a genotype-blinded manner.

2.4. SDS-polyacrylamide gel electrophoresis (PAGE) and Western blotting

SDS-PAGE and Western blotting were carried out as previously described (Huang et al., 2008). Samples of fresh or cultured macrophages were washed with phosphate-buffered saline (PBS) and lysed in SDS-PAGE sample buffer containing 2% SDS. Total protein was extracted by sonication and heated at 80°C for 5 min. Urinary bladder tissues were examined to verify genotypes and the SDS-PAGE samples were prepared similarly, in which the extraction of protein was done with mechanical homogenization.

The protein extracts were analyzed using 12% gel in Laemmli buffer system with an acrylamide:bisacrylamide ratio of 29:1. After electrophoresis, the gels were fixed and stained with Coomassie Blue R-250 to verify sample integrity and normalize protein input. Duplicated gels were electrically blotted on nitrocellulose membrane using a Bio-Rad semi-dry transfer apparatus for Western blot analysis. The membrane was incubated with a rabbit antiserum, RAH2, which was raised against mouse calponin 2 immunogen and has weaker cross-reaction to calponin 1 (Nigam et al., 1998) or a mouse anti-calponin 1 monoclonal antibody (mAb) CP1 (Jin et al., 1996) in Tris-buffered saline containing 0.1% bovine serum albumin (BSA). The calponin bands recognized by the first antibody were revealed using alkaline phosphatase-labeled anti-rabbit IgG or anti-mouse IgG second antibody (Santa Cruz

Biotechnology) and 5-bromo-4-chloro-3-indolyl phosphate/nitro blue tetrazolium chromogenic substrate reaction.

2.5. *In vitro* wound healing assay

Elicited mouse peritoneal macrophages were seeded in glass-bottom dishes (P35G-0-14-C, MatTek) at 1.5×10^6 per microwell for adhesion at high-density. Foam cells were produced by incubating the adhered macrophages with 50 μg/mL acetylated LDL for 24 hours. The monolayers of confluent macrophages and foam cells were wounded by scratching using a thin pipette tip. Care was taken to produce uniformly sized wounds of approximately 300 μm in width. The detached cells were washed away with culture medium containing 10% FBS.

The scratch-wounded monolayer cultures were incubated in 5% CO_2 at 37°C in a stage top incubator (Model TC-124A, Warner Instruments) mounted on an inverted microscope (Zeiss Axiovert 100, Germany). Closure of the wound was monitored using an attached digital camera (AmScope). The wound area of each recorded field was measured using ImageJ64 MRI wound healing and ROI tools (NIH, Bethesda, MD). The assay was performed in a genotype-blinded manner.

2.6. Examination and quantification of aortic atherosclerotic lesions

6.5-month-old male and female mice were studied. Lesion development in the aortae was determined using the *en face* method (Bjorklund et al., 2014). The entire aorta was removed, cleaned for periadventitial fat and carefully cut open longitudinally. The opened aorta was then pinned on a dark color board and stained with 60% Oil Red O at room temperature for 50 minutes. The aorta tissue was examined under a dissection scope and photographed. The images were analysis with ImageJ64 software. The area examined covered both thoracic and abdominal regions defined as the segment from 0.8 mm before the branch point of the innominate artery to the iliac bifurcation, including 0.5 mm of the large branching vessels at the aortic arch.

Atherosclerosis lesion at the aortic root was studied in tissue cross-sections. Briefly, the base of the heart including the most proximal part of the ascending aorta was excised and embedded in O.C.T. compound (Tissue-Tek, 4583). The tissue piece was oriented to have all three aortic valves in the same geometric plane. The portion containing the aortic root was cut consecutively into 8 μm sections, starting from the commissures of the aortic cusps, using a Leica CM 1950 cryostat. Sections were collected on Fisher Superfrost Plus-coated slides following a scheme similar to that described previously (Daugherty and Whitman, 2003), processed for Oil Red O, hematoxylin, and eosin stain after fixation in 3.7% formaldehyde. The slides were imaged and the aortic root lesion area was determined using ImageJ64 software.

2.7. Immunohistochemistry

Aortic root sections were fixed in 75% acetone with 25% ethanol for 10 min and blocked in PBS containing 0.05% Tween-20 and 1% BSA at room temperature for 30 min. Endogenous peroxidase was inactivated by incubation with 1% H_2O_2 in PBS at room temperature for 10

min. After wash with PBS, the sections were stained with a rat mAb against mouse CD68 (Bio-Rad MCA 1957) or normal rat serum control at room temperature for 2 hrs. After washing with PBS-Tween-20 to remove excess primary antibody, the sections were incubated with horseradish peroxidase-conjugated anti-rat secondary antibody (SouthernBiotech, 3050-05) at room temperature for 1 hr. Washed with PBS-Tween-20 again to remove excess secondary antibody, the labeling of CD68 was visualized via 3,3'-diaminobenzidine-H_2O_2 substrate reaction in a dark box for 1 min. The reaction was stopped by repeating washes with 20 mM Tris-HCl, pH 7.6. Nuclei were then counterstained with Hematoxylin. Slides were mounted with cover slips and imaged. The areas of macrophage infiltration were determined using ImageJ64 software.

2.8. Multiplexed cytokine analysis

Peritoneal residential macrophages were isolated from WT and *Cnn2*$^{-/-}$ mice as above and seeded in 24-well plates at 2×10^6 per well in RPMI 1640 medium containing 10% FBS. The adherent cells were cultured at 37°C in RPMI 1640 medium containing 10% FBS. Foam cells were produced by replacing the culture medium with RPMI 1640 containing 10% FBS and 100 μg/ml acetylated LDL. After 48 hrs of culture, the cells were gently washed twice with PBS and total protein contents were extracted with a lysis buffer containing 50 mM Tris-HCl, 150 mM NaCl, 0.5% IGEPAL CA-630 (Sigma I3021), 1 mM EDTA and protease inhibitor cocktail (13911, Sigma-Aldrich). After sitting on ice for 20 min, the cell lysates were transferred to centrifuge tubes and centrifuged in a microcentrifuge at 14,000 rpm, 4°C for 10 min. The clarified supernatant was collected and stored at −80°C.

Cytokine/chemokine levels in the samples were quantified using bead-based multiplex immunoassays at a commercial service facility (Eve Technologies). The assays utilized multiplex assay platforms. A standard curve was generated for the measurement range of our samples based on a pilot assay performed on our submitted samples. The measured cytokine/chemokine concentrations are related to the level of production as well as cell concentration of each sample, therefore the results were normalized to the level of total protein determined using SDS-PAGE densitometry.

2.9. Cell adhesion assay

Freshly isolated peritoneal residential cells from WT and *Cnn2*$^{-/-}$ mice were seeded in multiple 12-well plates at the density of 2.5×10^5 cells per well in 500 μl RPMI-1640 medium containing 10% FBS. The WT and *Cnn2*$^{-/-}$ cells were seeded on the same plate to ensure parallel washing conditions. At a series of time points, non-adherent cells were removed by gentle washing with pre-warmed RPMI-1640 medium for three times. The adherent cells were then fixed immediately in the wells with 1% glutaraldehyde for 30 min. A seeding control plate of cells was fixed directly without washing by adding 50 μl 11% glutaraldehyde into each well (for a final concentration of glutaraldehyde of 1%).

The fixed plates were washed three times by submersion in deionized water, air-dried, and stained by adding 500 μL of 0.1% Crystal Violet in 20 mM MES buffer, pH 6.0. After shaking at room temperature for 20 min, the plates were washed with deionized water to remove excess crystal violet dye and air-dried prior to solubilizing the bound dye in 120 μL

of 10% acetic acid. 100 μL of the dye extract was transferred from each well to a 96-well plate for quantification (Kueng et al., 1989). $A_{595\ nm}$ values were measured with a reference wavelength of 655 nm using a Bio-Rad Benchmark automated microplate reader. The experiments were done in triplicate wells and repeated.

2.10. Isolation and culture of mouse skin fibroblasts

Fibroblasts were isolated as described previously from the back skin of neonatal WT and *Cnn2*$^{-/-}$ mice (Sanford et al., 1948). Briefly, 3-4 days old mice were euthanized and soaked in 70% ethanol for 2 minutes before removing the skin around torso under sterile condition. In a 35 mm culture dish, the skin was incubated with 0.5% trypsin (9002-07-7 GIBCO) in DMEM at 37°C for 1 hr. After washing with DMEM, the tissue was minced into fine pieces using a sharp razor for digestion in 2 mL of 700 U/mL collagenase I (M3A14008A Worthington) in DMEM at 37°C for 2 hrs in a 15 mL centrifuge tube with agitation every 20 minutes by gentle shaking. 2 mL ice-cold DMEM containing 20% FBS was then added and the tube was vortex 5 seconds for 5 times. The tissue suspension was pipetted up and down several times and the isolated cells were passed through a 100 μm nylon mesh. The cells were collected by centrifugation at 150 × g for 5 minutes and re-suspend in 8 mL DMEM containing 20% FBS for culture at 37°C in 5% CO_2. Soon after becoming confluent, the P_0 cells from each mouse were expanded into four 100 mm dishes to prepare 8-10 vials of frozen stock of P_1 cells (0.5 to 1 million cells per vial). Urinary bladder of each mouse was examined using Western blot as above to verify the Cnn2$^{-/-}$ and WT genotypes. The frozen cells were stored in liquid nitrogen before being thawed and passed one more time (P_2) for experiments.

2.11. Immunofluorescence microscopy

Mouse skin fibroblasts and peritoneal macrophages were cultured on pre-cleaned glass coverslips. After adherent culture for 24 hrs, pre-confluent cells on the coverslips were fixed with cold acetone or 4% paraformaldehyde for 15 min. After blocking with 1% BSA in PBS at room temperature for 30 min (paraformaldehyde fixed cover slips were penetrated with 0.5% Triton X-100 for 10 min prior to blocking), the coverslips were incubated with anti-calponin 2 mAb 1D11 (Hossain et al., 2006), anti-calponin 2 rabbit polyclonal Ab RAH2 (Nigam et al., 1998), anti-tropomyosin mAb CG3 (Lin et al., 1988), anti-paxillin mAb 5H11 (EMD Millipore 05-417), and an anti-non-muscle myosin IIA rabbit polyclonal Ab (Abcam, ab24762) at 4°C overnight. After washes with PBS containing 0.05% Tween-20, the coverslips were stained with corresponded secondary antibodies: Fluorescein isothiocyanate (FITC)-conjugated goat anti-mouse IgG (Sigma, F1010), FITC-conjugated sheep anti-rabbit IgG (Sigma, F7512), tetramethylrhodamine isothiocyanate (TRITC)-conjugated goat anti-rabbit IgG (Sigma, T6778) and TRITC-conjugated phalloidin (Sigma P1951) (for actin filaments) at room temperature for 1 hr. After final washes with PBS containing 0.05% Tween-20, the coverslips were mounted on glass slides and examined using fluorescence confocal microscopy for the cellular localizations of calponin 2 in macrophages and fibroblasts in relationship to the other cytoskeleton proteins.

2.12. Data analysis

All quantitative data are presented as mean ± SEM. Statistical analysis was done with Student's test or two-way ANOVA using the Origin software (two-tailed assays unless noted in the figure legend).

3. Results

3.1. *Cnn2*$^{-/-}$ macrophages retain the ability of lipid uptake

Our previous studies demonstrated that *Cnn2*$^{-/-}$ macrophages have enhanced phagocytotic activity, which was assessed by the uptake of mouse serum-coated fluorescent latex beads (Huang et al., 2008). Different from the non-specific phagocytosis of beads, the uptake of lipid complex by macrophages is a scavenger receptor-mediated engulfment, and also related to the intracellular cholesterol metabolism in macrophages. Therefore, here we first examined whether deletion of calponin 2 affects the lipid uptake ability of macrophages. Peritoneal residential macrophages from *Cnn2*$^{-/-}$ and WT mice were studies and the formation of foam cells were examined after 4, 8 and 24 hrs of incubation with acetylated LDL. The results showed that intracellular lipid droplets were significantly increased during the course of incubation in both WT and *Cnn2*$^{-/-}$ groups. No significant difference was detected at any of the time points studied (Fig. 1).

3.2. Deletion of calponin 2 compensates for the impaired motility of lipid-laden foam cells

The intrinsic motility of calponin 2-null macrophages and foam cells were investigated in the absence of chemotactic stimulation. *In vitro* wound healing assay in monolayer cell cultures was used for measuring the rate of two-dimensional cell migration. To obtain confluent monolayer cultures, elicited peritoneal macrophages were used in the assay. The SDS-gel and Western blots in Fig. 2A demonstrated similar levels of calponin 2 expressed in residential and elicited mouse peritoneal macrophages. Fig. 2B further shows the effective lipid loading in the production of foam cells for use in the wound healing assays.

The wound healing studies showed a significantly faster closure of the scratch wound in *Cnn2*$^{-/-}$ macrophages versus the wild type control (Fig. 3A). This result is consistent with the faster than WT migration velocity of *Cnn2*$^{-/-}$ macrophages measured on individual cells by tracking cell movement using time-lapse microscopy (Huang et al., 2016). The migration velocities of WT and *Cnn2*$^{-/-}$ foam cells were both significantly hindered as compared to that of the genotype-matched macrophages. However, the migration velocity of WT foam cells was hindered significantly more than that of *Cnn2*$^{-/-}$ foam cells. As a consequence, *Cnn2*$^{-/-}$ foam cells moved even faster than that of WT macrophages (Fig. 3B).

3.3. Deletion of calponin 2 attenuated the development of atherosclerosis in *ApoE*$^{-/-}$ mice

Apolipoprotein E (ApoE) is present on the surface of several lipoproteins and plays an important role in cholesterol transportation and metabolism. ApoE deficiency in mice leads to hyperlipidemia and spontaneous atherosclerosis even when fed with a normal diet (Daugherty, 2002). To focus our study on the effect of calponin 2 deletion on the function of macrophages in the pathogenesis of atherosclerosis under a relatively more physiological condition, ApoE$^{-/-}$ mice fed on a normal chow diet was used as the atherosclerosis model.

*Apo*E$^{-/-}$; *Apo*E$^{-/-}$,*Cnn2*$^{-/-}$ double KO and *ApoE*$^{-/-}$,*Cnn2*$^{f/f}$,*lysM*$^{cre+}$ myeloid-specific *Cnn2* KO mice *were studied* at 6.5 month of age to examine aortic atherosclerotic lesions. A possible gender difference in the development of atherosclerosis in *Apo*E$^{-/-}$ mice has been suggested (Tangirala et al., 1995; Coleman et al., 2006) (Chiba et al., 2011) (Meyrelles et al., 2011). Therefore, data of both male and female were collected in our study to consider gender-based variation. The aorta *en face* method was employed and atherosclerotic lesions were quantified.

While no significant difference was detected in the levels of total serum cholesterol between *ApoE*$^{-/-}$ and *ApoE*$^{-/-}$,*Cnn2*$^{-/-}$ mice (537±157 mg/dL and 519±176 mg/dL, respectively (mean ± SE, P=0.79), the results in Fig. 4 showed that in male mice, the area of *Apo*E deficiency-caused atherosclerotic plaques was reduced by 56.2% with global deletion of calponin 2 and by 91.9% with myeloid cell-specific deletion of calponin 2. In females, *ApoE*$^{-/-}$,*Cnn2*$^{-/-}$ and *ApoE*$^{-/-}$,*Cnn2*$^{f/f}$,*lysM*$^{cre+}$ mice also showed significantly reduced plaque areas (*51.9%* and *50.3%* less as compared with that in *ApoE*$^{-/-}$ controls, respectively). We further examined the atherosclerotic lesions at aortic roots of male *ApoE*$^{-/-}$,*Cnn2*$^{f/f}$,*lysM*$^{cre+}$ mice and *ApoE*$^{-/-}$ controls. The results in Fig. 5 showed significantly less total lesion area and macrophage content in *ApoE*$^{-/-}$,*Cnn2*$^{f/f}$,*lysM*$^{cre+}$ mice.

The fact that myeloid cell-specific KO of *Cnn2* has the same or stronger effect in comparison with that of global KO indicates that the therapeutic effect was primarily via the function of myeloid cells. This result is also consistent with our recent finding that myeloid cell-specific *Cnn2* KO had stronger effects on attenuating inflammatory arthritis than that of global *Cnn2* KO (Huang et al., 2016). These data indicate that the loss of calponin 2 in some other cell types may counteract the effect of calponin 2 deletion in myeloid cells on the attenuation and resolution of inflammation.

LysM-cre induces targeting of *Cnn2* in macrophages as well as other myeloid cells. We recently showed that *Cnn2* KO did not alter the subsets of Ly6C^{hi} and Ly6C^{low} monocytes, which are considered the sources of inflammatory and anti-inflammatory macrophages, respectively. No subset difference was detected in peritoneal residential macrophages from WT and *Cnn2*$^{-/-}$ mice (Huang et al., 2016). These data support that *Cnn2* KO in myeloid cells attenuates the pathogenesis of atherosclerosis via post-monocyte mechanisms.

It was reported that endogenous estrogen plays an atheroprotective role in female mice (Thomas and Smart, 2007). However, there are also data indicating that the lesions in *ApoE*$^{-/-}$ mice were severer in females (Caligiuri et al., 1999) (Meyrelles et al., 2011). Our present study showed severer lesion development in female *ApoE*$^{-/-}$ mice and a likely more effective attenuation of atherosclerosis by calponin 2 deletion in male mice (Fig. 4B). The significance of this observation merits investigation in future studies.

3.4. Deletion of calponin 2 alters cytokine productions of macrophages and foam cells

Cnn2$^{-/-}$ and WT mouse macrophages and *in vitro* lipid-loaded foam cells were examined for their production of cytokines. The quantitative data in Fig. 6A and the summary heat map in Fig. 6B demonstrated that in comparison with untreated WT macrophages, WT foam

cells had increases in cytokines associated with monocytosis (M-CSF and IL-3) and inflammation (IL-1α and VEGF). On the other hand, untreated *Cnn2*$^{-/-}$ macrophages exhibited decreased baseline levels of cytokines associated with monocytosis (G-CSF and M-CSF) and inflammation (IL-6, IFN-γ and CXCL10) as compared with that of untreated WT macrophages. In comparison with that of WT foam cells, *Cnn2*$^{-/-}$ foam cells had significantly lower levels of cytokines associated with monocytosis (Eotaxin, G-CSF, M-CSF and IL-3) and inflammation (IL-6, IL-12, IFN-γ, CXCL10, CXCL1, TNF-α and VEGF).

3.5. Deletion of calponin 2 decreases adhesion of macrophages to culture substrate

It is known that calponin 2 plays a role in enhancing the adhesion of cells to culture substrate (Hossain et al., 2014). Substrate adhesion is a critical factor in macrophage differentiation and activation (Liu et al., 2008). The results in Fig. 7 showed that the deletion of calponin 2 significantly weakened and slowed adhesion of macrophages to the culture substrate, suggesting a possible mechanism for calponin 2 to regulate macrophage functions via altering cell adhesion.

To investigate the mechanism for calponin to regulate cell adhesion, primary skin fibroblasts were studied taking advantage of their extended spreading in culture, which permits more clear imaging of the cytoskeleton. Typical actin stress fibers were seen in the cultured neonatal mouse skin fibroblasts (Fig. 8). Immunofluorescence staining using anti-calponin 2 mAb 1D11 and rabbit polyclonal antibody RAH2 revealed co-localizations of calponin 2 with F-actin, tropomyosin and myosin IIA, but not with paxillin-stained focal adhesions (Turner, 2000). The results suggest that calponin 2 enhances substrate adhesion of cells possibly by decreasing dynamics of the actin cytoskeleton through the inhibition of myosin motor function, which is a fundamental function of calponin (Shirinsky et al., 1992) (Haeberle, 1994).

3.6. Intracellular distribution of calponin 2

We further examined the effect of calponin 2 deletion on the actin-myosin cytoskeleton in WT and *Cnn2*$^{-/-}$ macrophages and foam cells. The results in (Fig. 9) showed that while F-actin is concentrated in the leading edge and the trailing tail of migrating macrophages, myosin mainly in the center of cell body. The distribution patterns of F-actin and myosin are similar in WT vs. *Cnn2*$^{-/-}$ macrophages and the foam cells. The cellular location of calponin 2 in WT macrophages and foam cells is similar to that of myosin IIA. A hypothesis is that calponin 2 enhances substrate adhesion of cells by inhibiting myosin motor function and decreasing dynamics of the cytoskeleton, which merits further investigation.

4. Discussion

Atherosclerosis is an inflammatory disease and the main cause of coronary heart disease and stroke (Libby, 2012). Macrophages play a central role in the pathophysiology of atherosclerosis and the regulation of macrophage function is a promising therapeutic target for the disease (Dickhout et al., 2008). In the present study, we investigated the role of calponin 2, an actin cytoskeleton-associated regulatory protein, in macrophages in the

development of arterial atherosclerosis. The results demonstrated that deletion of calponin 2 enhances the motility of macrophages, compensates for the hindered motility of foam cells (Fig. 3), and attenuates the development of ApoE deficiency-caused atherosclerosis in vivo (Figs. 4 and 5). These novel findings have several impacts on our understanding of calponin regulation of macrophage function in inflammatory diseases.

4.1. Deletion of calponin 2 increases the motility of macrophages and compensates for the impaired motility of foam cells

Macrophages and foam cells are pivotal cell types in the development of inflammatory lesion in arterial atherosclerosis, effecting on the progression and regression of plaques (Moore et al., 2013). Although phagocytosis clearance of lipoproteins by macrophages is likely to be beneficial at the outset of this inflammatory response, dysregulation of lipid metabolism and accumulation of lipid-ingested macrophages in atherosclerotic plaques may alter immune phenotypes and cause apoptosis to exaggerate inflammatory response and aggravate the progression of atherosclerosis lesion. Therefore, promotions of cholesterol efflux from macrophages (Ohashi et al., 2005) and macrophage emigration from plaques (van Gils et al., 2012) have been proposed as therapeutic approaches.

Cholesterol loading in macrophages results in significant reduction of migration ability (Pataki et al., 1992) (Qin et al., 2006), accompanied by decreased capacity of force generation by cell locomotors (Zerbinatti and Gore, 2003). Lipid-ingested macrophages have hindered migration and the retention of macrophages in atherosclerotic lesions contributes to the failure of resolving inflammation and plaque development (Ludewig and Laman, 2004) (Moore et al., 2013). Reversal of cholesterol loading can restore the migration ability of macrophages (Qin et al., 2006). Calponin 2 is a regulator of cell motility. Calponin binds to F-actin and inhibits the actin-activated MgATPase activity of myosin II (Winder and Walsh, 1990) (Abe et al., 1990). This function plays a role in modulating smooth muscle contractility and corresponds to the effect of calponin 2 on stabilizing the actin cytoskeleton in non-muscle cells and inhibiting cell motility (Liu and Jin, 2016). Calponin 2 and myosin II are both concentrated in the center of the cell body of macrophages (Fig. 9), supporting this hypothesis that deletion of calponin 2 removes an inhibition of myosin II motor and increases the dynamics of the cytoskeleton. This mechanism lays a foundation for calponin to regulate actin cytoskeleton-based functions, such as cell proliferation, adhesion and migration (Hossain et al., 2003) 2014; Liu & Jin 2016).

Previous studies have demonstrated that primary fibroblasts and peritoneal macrophages isolated from *Cnn2*$^{-/-}$ mice migrated faster than that of WT control cells (Hossain et al.) (Huang et al., 2008). Our present study further showed that deletion of calponin 2 increases the motility of not only macrophages but also foam cells, overcoming the negative impact of lipid loading (Fig. 3). Since *Cnn2*$^{-/-}$ and WT macrophages have similar amount of lipid loading (Fig. 1), the less impaired motility of *Cnn2*$^{-/-}$ foam cells is likely based on higher intrinsic cytoskeleton dynamics other than increasing lipid efflux. This notion is supported by the fact that the motility of *Cnn2*$^{-/-}$ foam cells remained faster than that of WT macrophages (Fig. 3).

This finding suggests that calponin 2 is a potential target for controlling the motility of macrophages and foam cells to attenuate the progression of atherosclerosis. Deleting calponin 2 to increase the motility of macrophages and compensate for the hindered motility of foam cells is a mechanism downstream of cellular signaling pathways, which may provide a specific treatment for atherosclerosis. Supporting this notion, the development of atherosclerosis in *ApoE*$^{-/-}$ mice was very effectively attenuated by deleting calponin 2 in macrophages (Figs. 4 and 5).

4.2. Deletion of calponin 2 in macrophages attenuates the development of atherosclerosis with reduced production of inflammatory cytokines

Cytokine-mediated cell signaling plays dominant roles during the pathogenesis and progression of atherosclerosis (Ramji and Davies, 2015). As expected, our study found up-regulations of pro-inflammatory cytokines M-CSF, IL-3, IL-1α and VEGF were found in WT foam cells compared to that in WT macrophages (Fig. 6). IL-1α is a prominent pro-inflammatory cytokine produced by macrophages following ingestion of oxidized LDL (Kamari et al., 2011; Freigang et al., 2013). Atherosclerotic lesions in *ApoE*$^{-/-}$ mice transplanted with *IL-1*α$^{-/-}$ bone marrow cells was 52% less than that in *IL-1*α$^{+/+}$ transplanted controls (Kamari et al., 2011). Atherosclerosis development is also accompanied by the up-regulation of VEGF (Kimura et al., 2007). VEGF stimulates the proliferation and growth of endothelial cells, induces angiogenesis, and potentially promotes plaque formation and destabilization (Holm et al., 2009). M-CSF and IL-3, cytokines that are associated with monocytosis, are induced by hypercholesterolemia and cause proliferation of hematopoietic stem cells and progenitor cells (Yvan-Charvet et al., 2010).

Our study further showed that the deletion of calponin 2 alters cytokine production profiles of macrophages and foam cells (Fig. 6). Comparing with WT foam cells, *Cnn2*$^{-/-}$ foam cells have decreased productions of monocytosis associated cytokines G-CSF, M-CSF and IL-3 and pro-inflammatory cytokines IL-6, and IFN-γ. The decreased production of inflammatory cytokines was also found in *Cnn2*$^{-/-}$ macrophages as compared to that in WT macrophages, indicating a baseline anti-inflammatory phenotype that effectively overrides the pro-inflammatory stimulation of lipid ingestion. This mechanism provides a molecular basis for the attenuated development of atherosclerosis in *Apo*E$^{-/-}$,*Cnn2*$^{-/-}$ and *Apo*E$^{-/-}$,*Cnn2*$^{f/f}$,*lysM*$^{cre+}$ mice (Figs. 4 and 5).

4.3. Deletion of calponin 2 decreases cell adhesion as a potential mechanism to reduce pro-inflammatory activity of macrophages

Calponin is an actin filament-associated regulatory protein and its function has been most extensively studied for the regulation of smooth muscle contractility (Liu & Jin, 2016). The smooth muscle-specific isoform calponin 1 functions as an inhibitory regulator of smooth muscle contraction through inhibiting actomyosin ATPase (Takahashi et al., 1988). Calponin 2 is the isoform of calponin expressed in macrophages and functions in decreasing the dynamics of actin cytoskeleton and regulating phagocytosis, migration and adhesion. The current knowledge regarding macrophage differentiation and functions in inflammatory diseases is mainly from studies of receptor-ligation based signaling pathways. Our present study showed that calponin 2, a cytoskeleton regulatory protein, effectively modifies the

function of macrophages in the development of atherosclerosis, proposing a novel cell motility-based mechanism to attenuate inflammatory diseases.

Differentiation and phenotype polarization of macrophages could promote either resolution of inflammatory process and attenuation of atherogenesis (Sharma et al., 2012) (Cardilo-Reis et al., 2012) or acceleration of atherosclerosis (Hanna et al., 2012) (Hamers et al., 2012). It has been broadly observed that substrate adhesion is critical for macrophage differentiation (Szekanecz and Koch, 2007) (Liu et al., 2008). Macrophages cultured on stiffer substrate exhibited increased spreading area and enhanced adhesion, accompanied with elevated classical activation than that of macrophages cultured on softer substrate (Blakney et al., 2012). Macrophage grown on soft substrates produced less proinflammatory cytokines with decreased TLR4 activity than that of the macrophages grown on rigid substrates (Previtera and Sengupta, 2015). The modulation of macrophage function by substrate rigidity is dependent on actin polymerization and RhoGTPase activation (Patel et al., 2012).

Similar to the findings in other cell types (Hossain et al.; Hines et al., 2014; Hossain et al., 2014), calponin 2 facilitates the adhesion of macrophages to the culture substrate (Fig. 7). Calponin 2 is not located at the cell focal adhesions but concentrated in the center of the cell body as that of myosin II (Figs. 8 and 9). This observation suggests that calponin 2 facilitates and stabilizes cell adhesion by inhibiting myosin II motor and reducing the dynamics of cytoskeleton. The deletion of calponin 2 to increase the dynamics of actin cytoskeleton and weaken cell adhesion (Fig. 7) could be responsible for the decreased baseline production of pro-inflammatory cytokines in $Cnn2^{-/-}$ macrophages and the attenuated up-regulation of pro-inflammatory cytokines in $Cnn2^{-/-}$ foam cells (Fig. 6).

5. Summary

Our study demonstrated that calponin 2 regulates macrophage function in the development of atherosclerosis via modulating the function of actin cytoskeleton. Deletion of calponin 2 increases macrophage motility and compensates for the impaired motility of foam cells, reduces inflammatory cytokines in macrophages and foam cells, and reduces atherosclerosis lesions in $ApoE^{-/-}$ mice. The data provide evidence that changes in myosin motor-based cytoskeleton dynamics and cell adhesion alter macrophage activities, implicating a potentially novel therapeutic target for the treatment and prevention of atherosclerosis.

Acknowledgement

We thank Ms. Hui Wang for technical assistance, and Taylor Heilig and Sienna Wong for PCR genotyping of the genetically modified mice.

Sources of funding

This study was supported by a grant from the National Institutes of Health AR-048816 to J-PJ.

References

Abe M, Takahashi K, Hiwada K. Effect of calponin on actin-activated myosin ATPase activity. J Biochem. 1990; 108:835–8. [PubMed: 2150518]

Bjorklund MM, Hollensen AK, Hagensen MK, Dagnaes-Hansen F, Christoffersen C, Mikkelsen JG, Bentzon JF. Induction of atherosclerosis in mice and hamsters without germline genetic engineering. Circ Res. 2014; 114:1684–9. [PubMed: 24677271]

Blakney AK, Swartzlander MD, Bryant SJ. The effects of substrate stiffness on the in vitro activation of macrophages and in vivo host response to poly(ethylene glycol)-based hydrogels. J Biomed Mater Res A. 2012; 100:1375–86. [PubMed: 22407522]

Caligiuri G, Nicoletti A, Zhou X, Tornberg I, Hansson GK. Effects of sex and age on atherosclerosis and autoimmunity in apoE-deficient mice. Atherosclerosis. 1999; 145:301–8. [PubMed: 10488957]

Cardilo-Reis L, Gruber S, Schreier SM, Drechsler M, Papac-Milicevic N, Weber C, Wagner O, Stangl H, Soehnlein O, Binder CJ. Interleukin-13 protects from atherosclerosis and modulates plaque composition by skewing the macrophage phenotype. EMBO Mol Med. 2012; 4:1072–86. [PubMed: 23027612]

Chiba T, Ikeda M, Umegaki K, Tomita T. Estrogen-dependent activation of neutral cholesterol ester hydrolase underlying gender difference of atherogenesis in apoE−/− mice. Atherosclerosis. 2011; 219:545–51. [PubMed: 21944698]

Chinetti-Gbaguidi G, Colin S, Staels B. Macrophage subsets in atherosclerosis. Nat Rev Cardiol. 2015; 12:10–7. [PubMed: 25367649]

Clausen BE, Burkhardt C, Reith W, Renkawitz R, Forster I. Conditional gene targeting in macrophages and granulocytes using LysMcre mice. Transgenic Res. 1999; 8:265–77. [PubMed: 10621974]

Coleman R, Hayek T, Keidar S, Aviram M. A mouse model for human atherosclerosis: long-term histopathological study of lesion development in the aortic arch of apolipoprotein E-deficient (E0) mice. Acta Histochem. 2006; 108:415–24. [PubMed: 17007910]

Daugherty A. Mouse models of atherosclerosis. Am J Med Sci. 2002; 323:3–10. [PubMed: 11814139]

Daugherty A, Whitman SC. Quantification of atherosclerosis in mice. Methods Mol Biol. 2003; 209:293–309. [PubMed: 12357958]

Dickhout JG, Basseri S, Austin RC. Macrophage function and its impact on atherosclerotic lesion composition, progression, and stability: the good, the bad, and the ugly. Arterioscler Thromb Vasc Biol. 2008; 28:1413–5. [PubMed: 18650503]

Freigang S, Ampenberger F, Weiss A, Kanneganti TD, Iwakura Y, Hersberger M, Kopf M. Fatty acid-induced mitochondrial uncoupling elicits inflammasome-independent IL-1alpha and sterile vascular inflammation in atherosclerosis. Nat Immunol. 2013; 14:1045–53. [PubMed: 23995233]

Haeberle JR. Calponin decreases the rate of cross-bridge cycling and increases maximum force production by smooth muscle myosin in an in vitro motility assay. J Biol Chem. 1994; 269:12424–31. [PubMed: 8175648]

Hamers AA, Vos M, Rassam F, Marinkovic G, Kurakula K, van Gorp PJ, de Winther MP, Gijbels MJ, de Waard V, de Vries CJ. Bone marrow-specific deficiency of nuclear receptor Nur77 enhances atherosclerosis. Circ Res. 2012; 110:428–38. [PubMed: 22194623]

Hanna RN, Shaked I, Hubbeling HG, Punt JA, Wu R, Herrley E, Zaugg C, Pei H, Geissmann F, Ley K, Hedrick CC. NR4A1 (Nur77) deletion polarizes macrophages toward an inflammatory phenotype and increases atherosclerosis. Circ Res. 2012; 110:416–27. [PubMed: 22194622]

Hines PC, Gao X, White JC, D'Agostino A, Jin JP. A novel role of h2-calponin in regulating whole blood thrombosis and platelet adhesion during physiologic flow. Physiol Rep. 2014:2.

Holm PW, Slart RH, Zeebregts CJ, Hillebrands JL, Tio RA. Atherosclerotic plaque development and instability: a dual role for VEGF. Ann Med. 2009; 41:257–64. [PubMed: 19089693]

Hossain MM, Crish JF, Eckert RL, Lin JJ, Jin JP. h2-Calponin is regulated by mechanical tension and modifies the function of actin cytoskeleton. J Biol Chem. 2005; 280:42442–53. [PubMed: 16236705]

Hossain MM, Hwang DY, Huang QQ, Sasaki Y, Jin JP. Developmentally regulated expression of calponin isoforms and the effect of h2-calponin on cell proliferation. Am J Physiol Cell Physiol. 2003; 284:C156–67. [PubMed: 12388067]

Hossain MM, Smith PG, Wu K, Jin JP. Cytoskeletal tension regulates both expression and degradation of h2-calponin in lung alveolar cells. Biochemistry. 2006; 45:15670–83. [PubMed: 17176089]

Hossain MM, Wang X, Bergan RC, Jin JP. Diminished expression of h2-calponin in prostate cancer cells promotes cell proliferation, migration and the dependence of cell adhesion on substrate stiffness. Febs Open Bio. 2014; 4:627–636.

Hossain MM, Zhao G, Woo M-S, Wang JHC, Jin JP. h2-calponin Gene Knockout Increases Traction Force of Mouse Fibroblasts in vitro. Biophysical Journal. 108:143a.

Huang QQ, Hossain MM, Sun W, Xing L, Pope RM, Jin JP. Deletion of calponin 2 in macrophages attenuates the severity of inflammatory arthritis in mice. Am J Physiol Cell Physiol. 2016:00331. in press. ajpcell. 2015.

Huang QQ, Hossain MM, Wu K, Parai K, Pope RM, Jin JP. Role of H2-calponin in regulating macrophage motility and phagocytosis. J Biol Chem. 2008; 283:25887–99. [PubMed: 18617524]

Jin JP, Walsh MP, Resek ME, McMartin GA. Expression and epitopic conservation of calponin in different smooth muscles and during development. Biochem Cell Biol. 1996; 74:187–96. [PubMed: 9213427]

Jin JP, Zhang Z, Bautista JA. Isoform diversity, regulation, and functional adaptation of troponin and calponin. Crit Rev Eukaryot Gene Expr. 2008; 18:93–124. [PubMed: 18304026]

Kamari Y, Shaish A, Shemesh S, Vax E, Grosskopf I, Dotan S, White M, Voronov E, Dinarello CA, Apte RN, Harats D. Reduced atherosclerosis and inflammatory cytokines in apolipoprotein-E-deficient mice lacking bone marrow-derived interleukin-1alpha. Biochem Biophys Res Commun. 2011; 405:197–203. [PubMed: 21219852]

Kimura K, Hashiguchi T, Deguchi T, Horinouchi S, Uto T, Oku H, Setoyama S, Maruyama I, Osame M, Arimura K. Serum VEGF--as a prognostic factor of atherosclerosis. Atherosclerosis. 2007; 194:182–8. [PubMed: 17141247]

Kueng W, Silber E, Eppenberger U. Quantification of cells cultured on 96-well plates. Anal Biochem. 1989; 182:16–9. [PubMed: 2604040]

Libby P. Inflammation in atherosclerosis. Arterioscler Thromb Vasc Biol. 2012; 32:2045–51. [PubMed: 22895665]

Lin JJ, Hegmann TE, Lin JL. Differential localization of tropomyosin isoforms in cultured nonmuscle cells. J Cell Biol. 1988; 107:563–72. [PubMed: 3047141]

Liu H, Shi B, Huang CC, Eksarko P, Pope RM. Transcriptional diversity during monocyte to macrophage differentiation. Immunol Lett. 2008; 117:70–80. [PubMed: 18276018]

Liu R, Jin JP. Calponin isoforms CNN1, CNN2 and CNN3: Regulators for actin cytoskeleton functions in smooth muscle and non-muscle cells. Gene. 2016; 585:143–53. [PubMed: 26970176]

Ludewig B, Laman JD. The in and out of monocytes in atherosclerotic plaques: Balancing inflammation through migration. Proc Natl Acad Sci U S A. 2004; 101:11529–30. [PubMed: 15292506]

Lusis AJ. Atherosclerosis. Nature. 2000; 407:233–41. [PubMed: 11001066]

Meyrelles SS, Peotta VA, Pereira TM, Vasquez EC. Endothelial dysfunction in the apolipoprotein E-deficient mouse: insights into the influence of diet, gender and aging. Lipids Health Dis. 2011; 10:211. [PubMed: 22082357]

Moore KJ, Sheedy FJ, Fisher EA. Macrophages in atherosclerosis: a dynamic balance. Nat Rev Immunol. 2013; 13:709–21. [PubMed: 23995626]

Nahrendorf M, Swirski FK. Immunology. Neutrophil-macrophage communication in inflammation and atherosclerosis. Science. 2015; 349:237–8. [PubMed: 26185231]

Nigam R, Triggle CR, Jin JP. h1- and h2-calponins are not essential for norepinephrine- or sodium fluoride-induced contraction of rat aortic smooth muscle. J Muscle Res Cell Motil. 1998; 19:695–703. [PubMed: 9742453]

Ohashi R, Mu H, Wang X, Yao Q, Chen C. Reverse cholesterol transport and cholesterol efflux in atherosclerosis. QJM. 2005; 98:845–56. [PubMed: 16258026]

Pataki M, Lusztig G, Robenek H. Endocytosis of oxidized LDL and reversibility of migration inhibition in macrophage-derived foam cells in vitro. A mechanism for atherosclerosis regression? Arterioscler Thromb. 1992; 12:936–44. [PubMed: 1637791]

Patel NR, Bole M, Chen C, Hardin CC, Kho AT, Mih J, Deng L, Butler J, Tschumperlin D, Fredberg JJ, Krishnan R, Koziel H. Cell elasticity determines macrophage function. PLoS One. 2012; 7:e41024. [PubMed: 23028423]

Piedrahita JA, Zhang SH, Hagaman JR, Oliver PM, Maeda N. Generation of mice carrying a mutant apolipoprotein E gene inactivated by gene targeting in embryonic stem cells. Proc Natl Acad Sci U S A. 1992; 89:4471–5. [PubMed: 1584779]

Previtera ML, Sengupta A. Substrate Stiffness Regulates Proinflammatory Mediator Production through TLR4 Activity in Macrophages. PLoS One. 2015; 10:e0145813. [PubMed: 26710072]

Qin C, Nagao T, Grosheva I, Maxfield FR, Pierini LM. Elevated plasma membrane cholesterol content alters macrophage signaling and function. Arterioscler Thromb Vasc Biol. 2006; 26:372–8. [PubMed: 16306428]

Ramji DP, Davies TS. Cytokines in atherosclerosis: Key players in all stages of disease and promising therapeutic targets. Cytokine Growth Factor Rev. 2015; 26:673–85. [PubMed: 26005197]

Ross R. Atherosclerosis--an inflammatory disease. N Engl J Med. 1999; 340:115–26. [PubMed: 9887164]

Sanford KK, Earle WR, Likely GD. The growth in vitro of single isolated tissue cells. J Natl Cancer Inst. 1948; 9:229–46. [PubMed: 18105872]

Sharma N, Lu Y, Zhou G, Liao X, Kapil P, Anand P, Mahabeleshwar GH, Stamler JS, Jain MK. Myeloid Kruppel-like factor 4 deficiency augments atherogenesis in ApoE−/− mice--brief report. Arterioscler Thromb Vasc Biol. 2012; 32:2836–8. [PubMed: 23065827]

Shibukawa Y, Yamazaki N, Daimon E, Wada Y. Rock-dependent calponin 3 phosphorylation regulates myoblast fusion. Exp Cell Res. 2013; 319:633–48. [PubMed: 23276748]

Shibukawa Y, Yamazaki N, Kumasawa K, Daimon E, Tajiri M, Okada Y, Ikawa M, Wada Y. Calponin 3 regulates actin cytoskeleton rearrangement in trophoblastic cell fusion. Mol Biol Cell. 2010; 21:3973–84. [PubMed: 20861310]

Shirinsky VP, Biryukov KG, Hettasch JM, Sellers JR. Inhibition of the relative movement of actin and myosin by caldesmon and calponin. J Biol Chem. 1992; 267:15886–92. [PubMed: 1639818]

Sosale NG, Spinler KR, Alvey C, Discher DE. Macrophage engulfment of a cell or nanoparticle is regulated by unavoidable opsonization, a species-specific 'Marker of Self' CD47, and target physical properties. Curr Opin Immunol. 2015; 35:107–12. [PubMed: 26172292]

Szekanecz Z, Koch AE. Macrophages and their products in rheumatoid arthritis. Curr Opin Rheumatol. 2007; 19:289–95. [PubMed: 17414958]

Takahashi K, Hiwada K, Kokubu T. Isolation and characterization of a 34,000-dalton calmodulin- and F-actin-binding protein from chicken gizzard smooth muscle. Biochem Biophys Res Commun. 1986; 141:20–6. [PubMed: 3606745]

Takahashi K, Hiwada K, Kokubu T. Vascular smooth muscle calponin. A novel troponin T-like protein. Hypertension. 1988; 11:620–6. [PubMed: 2455687]

Tang J, Hu G, Hanai J, Yadlapalli G, Lin Y, Zhang B, Galloway J, Bahary N, Sinha S, Thisse B, Thisse C, Jin JP, Zon LI, Sukhatme VP. A critical role for calponin 2 in vascular development. J Biol Chem. 2006; 281:6664–72. [PubMed: 16317011]

Tangirala RK, Rubin EM, Palinski W. Quantitation of atherosclerosis in murine models: correlation between lesions in the aortic origin and in the entire aorta, and differences in the extent of lesions between sexes in LDL receptor-deficient and apolipoprotein E-deficient mice. J Lipid Res. 1995; 36:2320–8. [PubMed: 8656070]

Thomas CM, Smart EJ. Gender as a regulator of atherosclerosis in murine models. Curr Drug Targets. 2007; 8:1172–80. [PubMed: 18045095]

Trabelsi-Terzidis H, Fattoum A, Represa A, Dessi F, Ben-Ari Y, der Terrossian E. Expression of an acidic isoform of calponin in rat brain: western blots on one- or two-dimensional gels and immunolocalization in cultured cells. Biochem J. 1995; 306(Pt 1):211–5. [PubMed: 7864813]

Turner CE. Paxillin and focal adhesion signalling. Nat Cell Biol. 2000; 2:E231–6. [PubMed: 11146675]

van Gils JM, Derby MC, Fernandes LR, Ramkhelawon B, Ray TD, Rayner KJ, Parathath S, Distel E, Feig JL, Alvarez-Leite JI, Rayner AJ, McDonald TO, O'Brien KD, Stuart LM, Fisher EA, Lacy-Hulbert A, Moore KJ. The neuroimmune guidance cue netrin-1 promotes atherosclerosis by inhibiting the emigration of macrophages from plaques. Nat Immunol. 2012; 13:136–43. [PubMed: 22231519]

Walsh MP. The Ayerst Award Lecture 1990. Calcium-dependent mechanisms of regulation of smooth muscle contraction. Biochem Cell Biol. 1991; 69:771–800. [PubMed: 1818584]

Winder SJ, Walsh MP. Smooth muscle calponin. Inhibition of actomyosin MgATPase and regulation by phosphorylation. J Biol Chem. 1990; 265:10148–55. [PubMed: 2161834]

Winder SJ, Walsh MP, Vasulka C, Johnson JD. Calponin-calmodulin interaction: properties and effects on smooth and skeletal muscle actin binding and actomyosin ATPases. Biochemistry. 1993; 32:13327–33. [PubMed: 8241189]

Wu KC, Jin JP. Calponin in non-muscle cells. Cell Biochem Biophys. 2008; 52:139–48. [PubMed: 18946636]

Yvan-Charvet L, Pagler T, Gautier EL, Avagyan S, Siry RL, Han S, Welch CL, Wang N, Randolph GJ, Snoeck HW, Tall AR. ATP-binding cassette transporters and HDL suppress hematopoietic stem cell proliferation. Science. 2010; 328:1689–93. [PubMed: 20488992]

Zerbinatti CV, Gore RW. Uptake of modified low-density lipoproteins alters actin distribution and locomotor forces in macrophages. Am J Physiol Cell Physiol. 2003; 284:C555–61. [PubMed: 12388112]

Zhang X, Goncalves R, Mosser DM. The isolation and characterization of murine macrophages. Curr Protoc Immunol. 2008 Chapter 14, Unit 14 1.

Highlights

- Deletion of calponin 2 in macrophages attenuates atherosclerosis in *ApoE*$^{-/-}$ mice
- Deletion of calponin 2 in macrophages facilitates migration and weakens adhesion
- *Cnn2*$^{-/-}$ macrophages and foam cells produce lower level of inflammatory cytokines
- Calponin 2 may be targeted to treat atherosclerosis and other inflammatory diseases

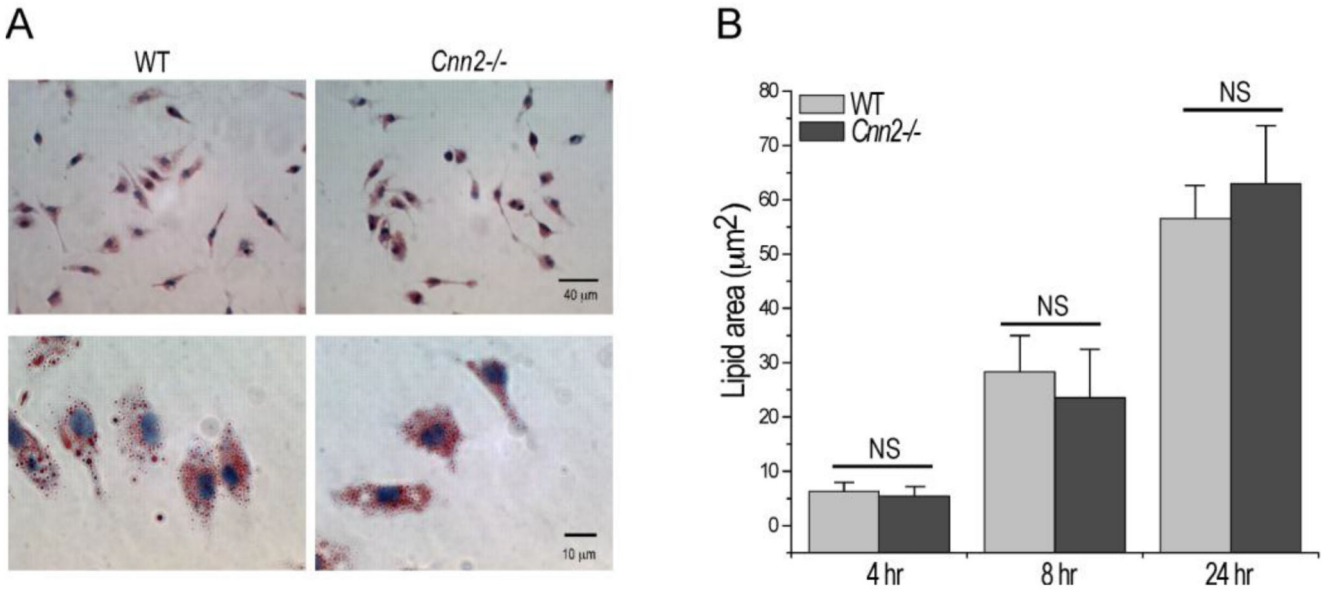

Figure 1. *Cnn2*$^{-/-}$ macrophages retained the ability of lipid engulfment and formation of foam cells

Peritoneal residential macrophages isolated from WT and *Cnn2*$^{-/-}$ mice were cultured on cover slips and incubated with 25 μg/ml acetylated LDL for 4, 8 and 24 hrs. Intracellular lipid droplets were stained with Oil Red O. The loading of lipids was highly effective: At 8 hrs 89.4±6.4% WT and 83.4±4.3% of Cnn2 KO macrophages engulfed lipid droplets, which increased to 97.7±2.3% and 91.6±0.9% at 24 hrs (mean ± SE). A. Representative low (upper panels) and high (lower panels) magnification images at 24 of hrs incubation with acetylated LDL. B. Quantitative measurements during the incubation with acetylated LDL. The results showed that the area and intensity of lipid droplets were significantly increased during the course of acetylated LDL incubation but no significant difference (NS) was detected between WT and *Cnn2*$^{-/-}$ groups (n=3 mice in each group).

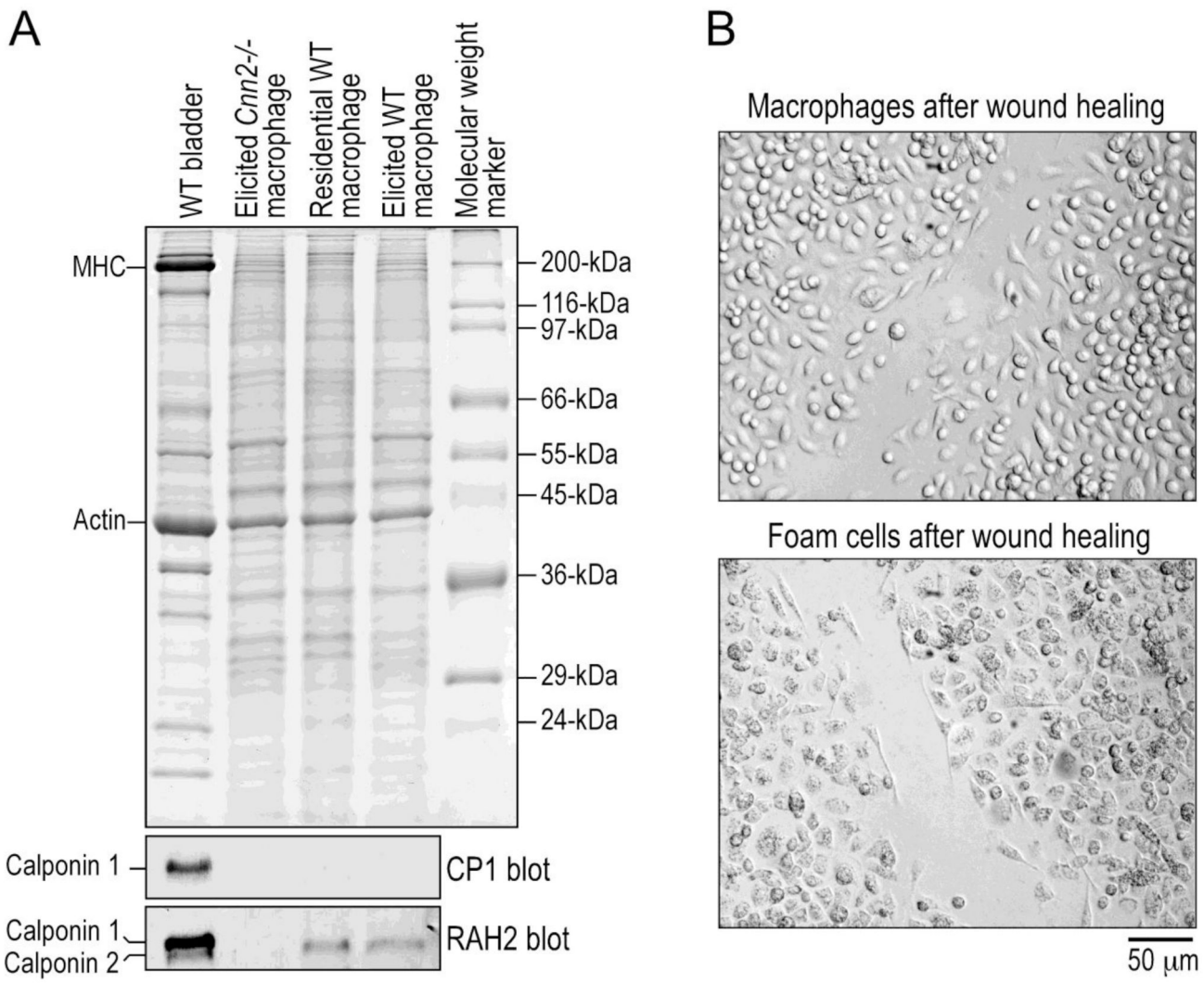

Figure 2. Similar levels of calponin 2 expression in residential and elicited mouse peritoneal macrophages and effective lipid loading to produce foam cells

SDS-PAGE and Western blots using mAb CP1 specifically against calponin 1 and polyclonal antibody RAH2 raised against calponin 2 showed similar levels of calponin 2 in residential and elicited mouse peritoneal macrophages. Wild type mouse urinary bladder that expresses both calponin 1 and calponin 2 was used as a positive control and *Cnn2*$^{-/-}$ macrophages as a negative control. No calponin 1 is detected in residential or elicited mouse peritoneal macrophages. B. The images *show a WT example for* acetylated LDL-treatment in culture to effectively transform all macrophages into foam cells (Fig. 1 showed that there is no difference in lipid ingestion between WT and Cnn2$^{-/-}$ macrophages), justifying their use in wound healing studies.

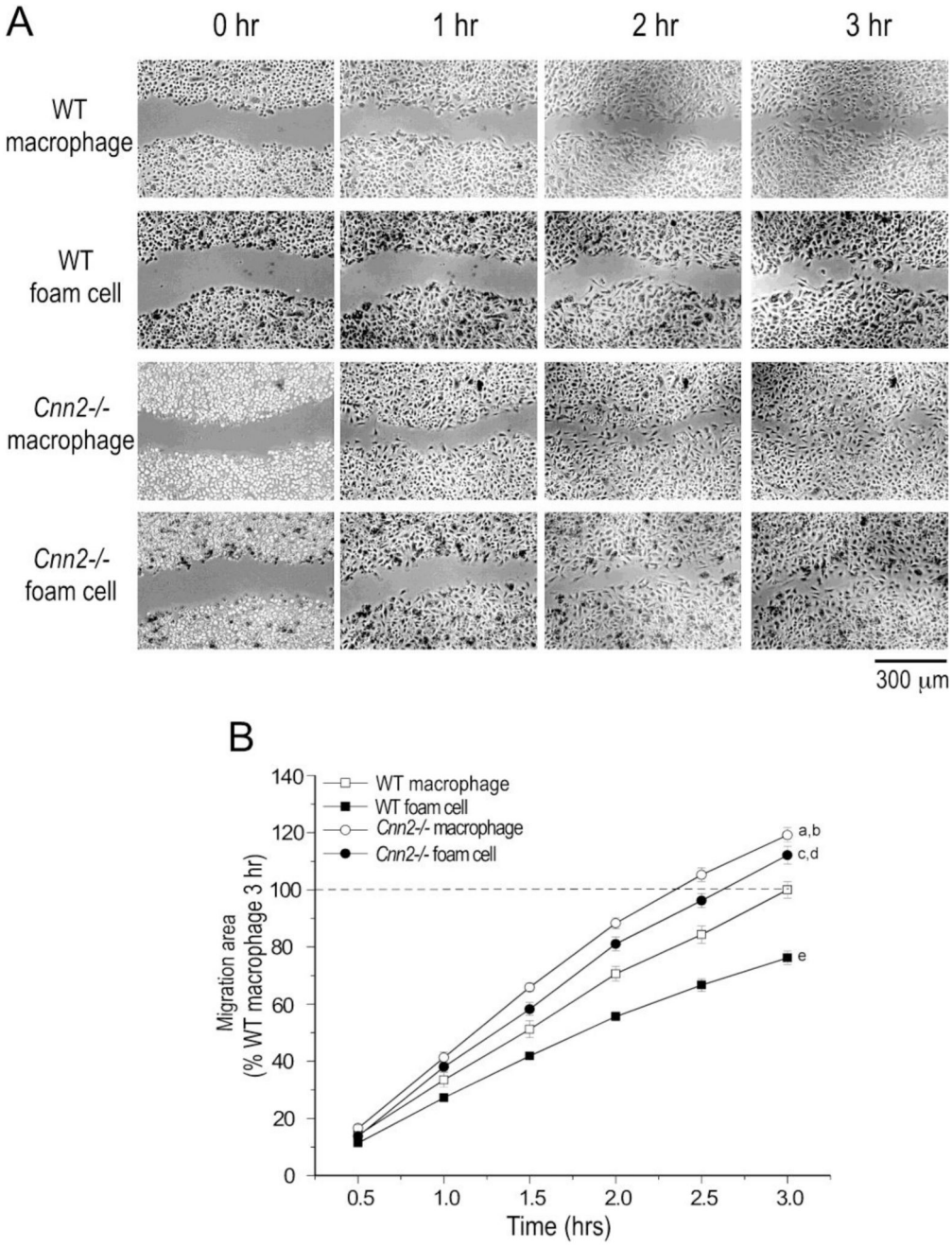

Figure 3. Faster migration of calponin 2-null macrophages than that of WT macrophages, compensating for the impaired migration of foam cells

Scratch wounds were made in monolayer cultures of mouse macrophages and foam cells. Healing of the wound by cell migration was monitored for 3 hrs. The micrographs (A) and densitometry quantification of the wound area (B) showed a faster closure of the wound in the *Cnn2*$^{-/-}$ macrophage culture than that of WT macrophage control. The migration velocity was hindered in both WT and *Cnn2*$^{-/-}$ foam cells as compared to that of genotype-matched macrophages, which was, however, significantly compensated in *Cnn2*$^{-/-}$ foam cells. Values are presented as Mean ± SEM. n equal to the experimental repeats (the number

of wounds studied in each of the Cnn2−/− and WT groups). [a]P<0.05, $Cnn2^{-/-}$ macrophage vs. WT macrophage; [b]P<0.05, $Cnn2^{-/-}$ macrophage vs. $Cnn2^{-/-}$ foam cell; [c]P<0.05, $Cnn2^{-/-}$ foam cell vs. WT foam cell; [d]P<0.05, $Cnn2^{-/-}$ foam cell vs. WT macrophage; [e]P<0.05 WT foam cell vs. WT macrophage. Statistical analysis was performed using two-way ANOVA with mean comparison using Tukey test.

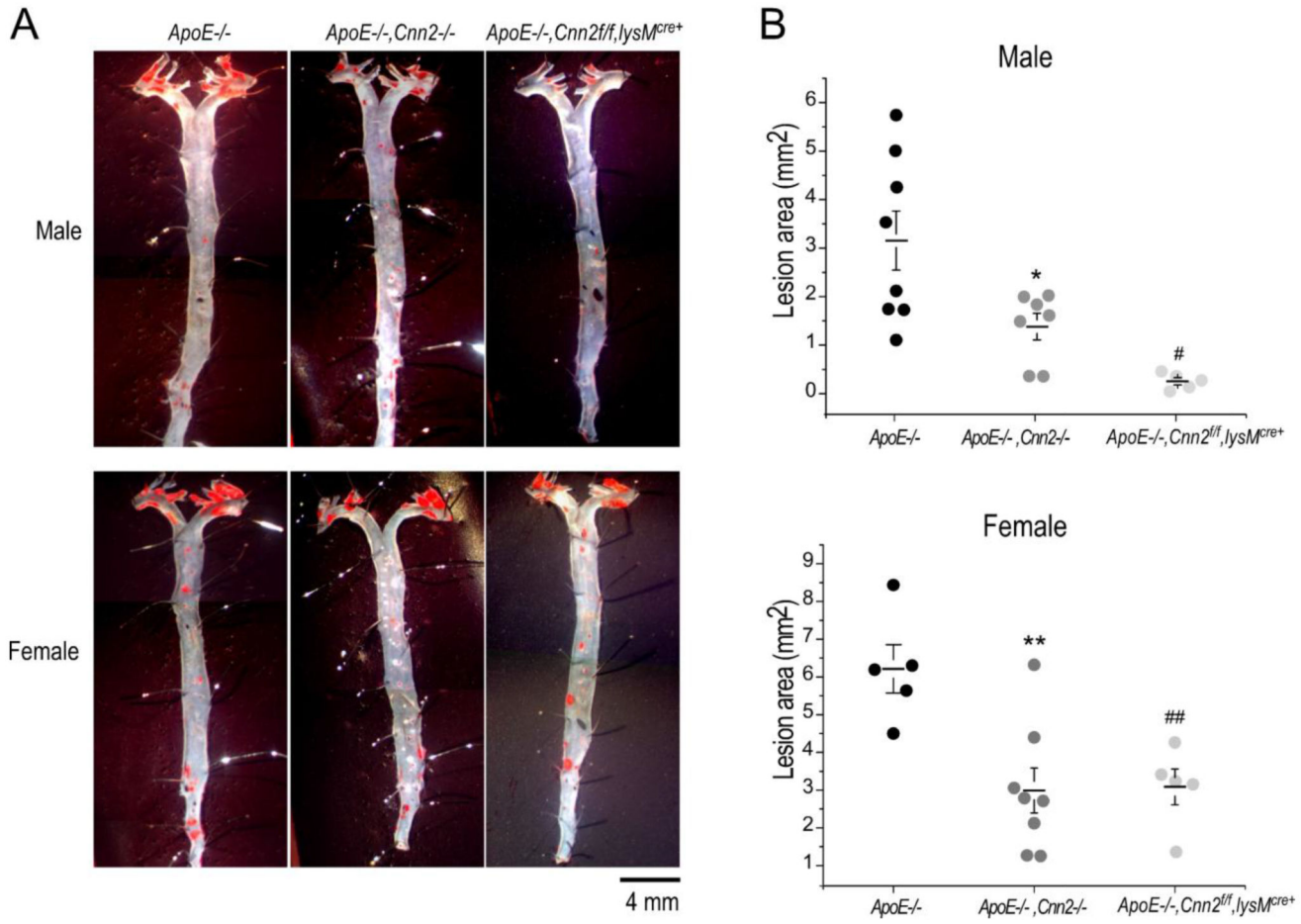

Figure 4. Atherosclerotic lesions in aorta *en face* of 6.5-month-old *ApoE*$^{-/-}$; *ApoE*$^{-/-}$,*Cnn2*$^{-/-}$ and *ApoE*$^{-/-}$,*Cnn2*$^{f/f}$,*lysM*$^{cre+}$ mice fed on standard chow diet

A. Representative Oil Red O staining of *en face* aorta. The results showed that *ApoE*$^{-/-}$,*Cnn2*$^{-/-}$ and *ApoE*$^{-/-}$,*Cnn2*$^{f/f}$, *lysM*$^{cre+}$ mice had significantly attenuated atherosclerotic lesions compared to that of the age- and sex-matched *ApoE*$^{-/-}$ mice. B. Lesion quantification of Oil Red O staining of *en face* aorta. **P*<0.05, *ApoE*$^{-/-}$,*Cnn2*$^{-/-}$ *vs.* *ApoE*$^{-/-}$; $^{\#}$*P*<0.05, *ApoE*$^{-/-}$,*Cnn2*$^{f/f}$,*lysM*$^{cre+}$ *vs.* *ApoE*$^{-/-}$; ***P*<0.01, *ApoE*$^{-/-}$,*Cnn2*$^{-/-}$ *vs.* *ApoE*$^{-/-}$; $^{\#\#}$*P*<0.01, *ApoE*$^{-/-}$,*Cnn2*$^{f/f}$,*lysM*$^{cre+}$ *vs.* *ApoE*$^{-/-}$.

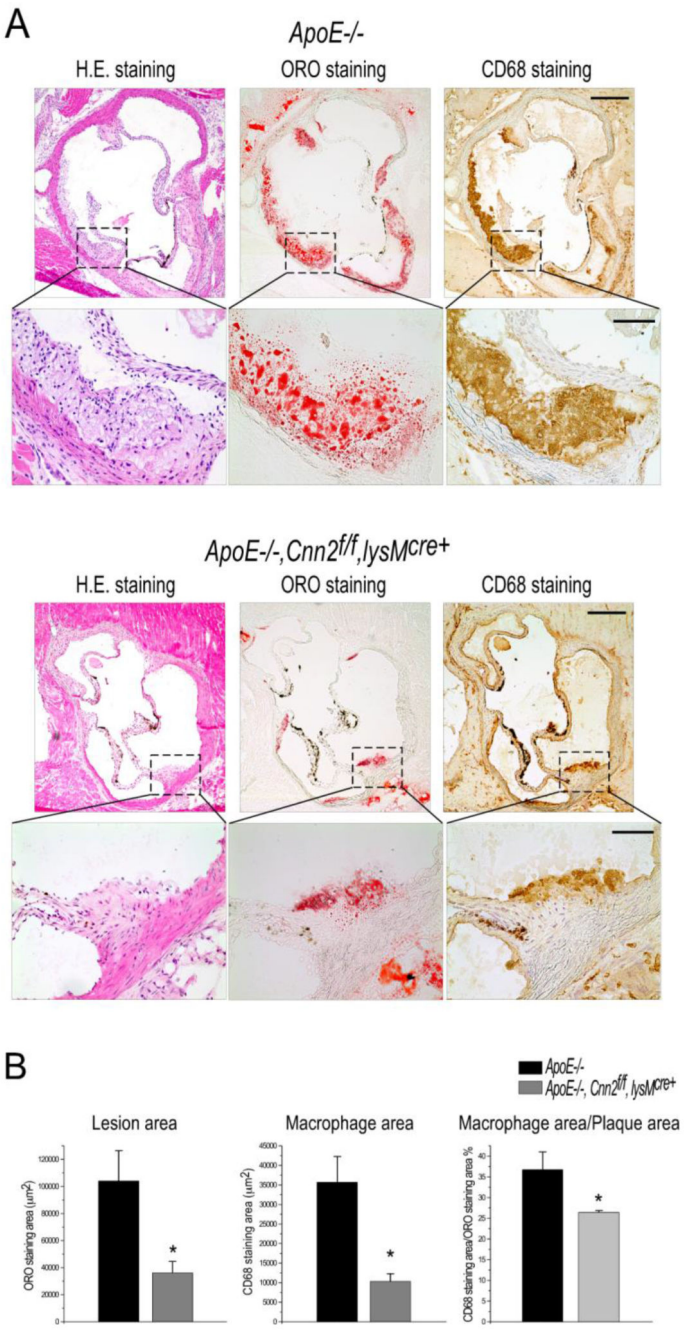

Figure 5. Atherosclerotic lesions in aortic root of 6.5-month-old ApoE$^{-/-}$ and ApoE$^{-/-}$,Cnn2$^{f/f}$,lysM^{cre+} mice fed on standard chow diet

A. Representative images of aortic sinus sections. Lesion morphology and lipid contents were evaluated with H & E and Oil Red O staining. Macrophage infiltration was detected via immunohistochemical staining for macrophage marker CD68. B. Quantification analysis of the lipid content and macrophage infiltration. The results showed that ApoE$^{-/-}$,Cnn2$^{f/f}$,lysM^{cre+} aortae had significantly attenuated atherosclerotic lesion and macrophage infiltration compared to that of age- and sex-matched ApoE$^{-/-}$ mice. *P<0.05.

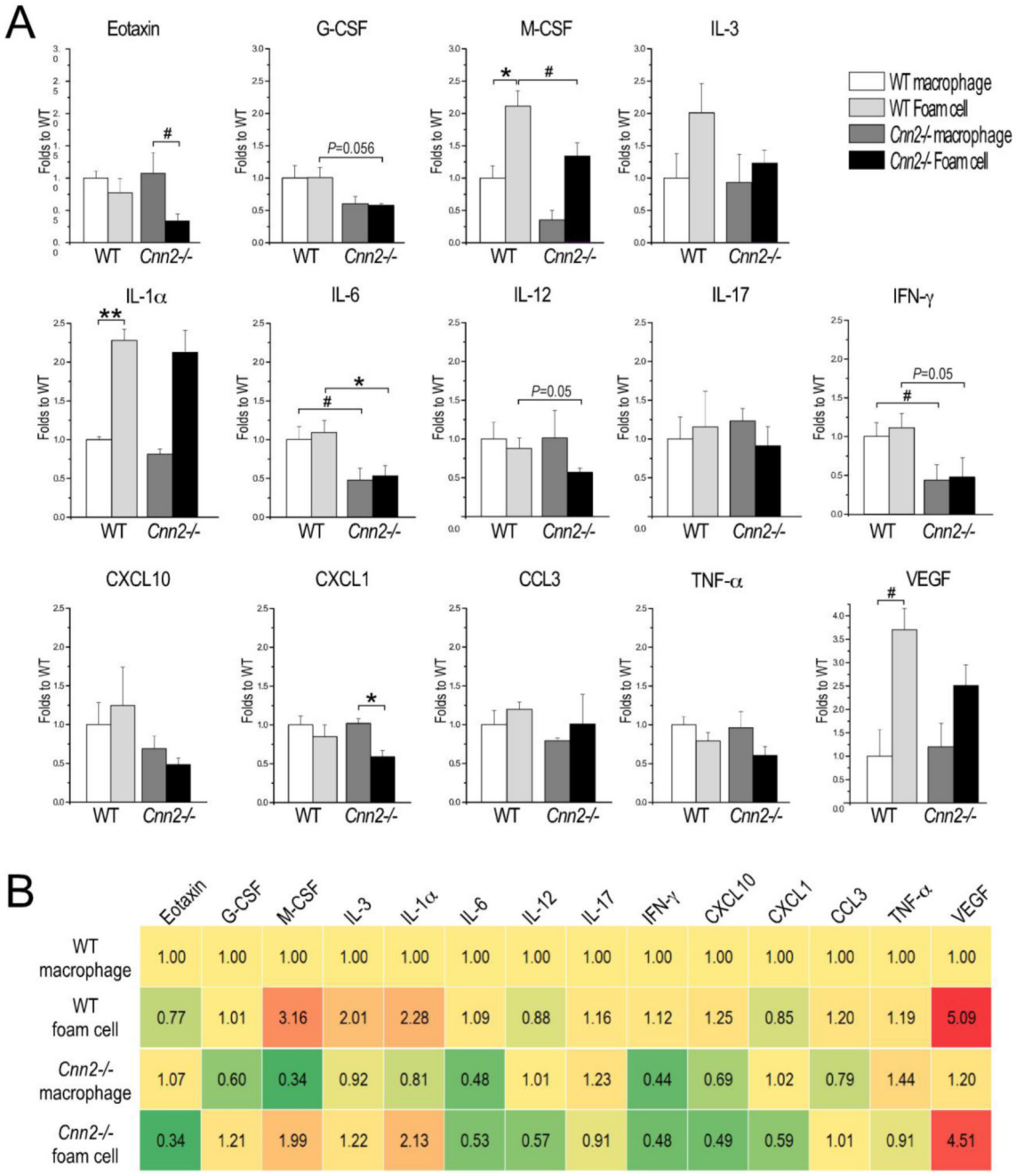

Figure 6. Cytokine production in WT and *Cnn2*$^{-/-}$ macrophages and foam cells

A. Levels of representative cytokines in WT and *Cnn2*$^{-/-}$ macrophages and foam cells. Values are presented as mean ± SEM (n=3 mice each for WT and *Cnn2*$^{-/-}$ groups). **P*<0.05, ***P*<0.01 (both two-tail *t*-test), and $^{\#}$*P*<0.05 (one-tail *t*-test). B. The heat map summarizes that WT foam cells had increases in cytokines associated with monocytosis (M-CSF and IL-3) and inflammation (IL-1α and VEGF) as compared with that of untreated WT macrophages. Untreated *Cnn2*$^{-/-}$ macrophages have decreased baseline levels of cytokines associated with monocytosis (G-CSF and M-CSF) and inflammation (IL-6, IFN-γ and

CXCL10) in comparison with that of untreated WT macrophages. *Cnn2*$^{-/-}$ foam cells also had significantly lower levels of cytokines associated with monocytosis (Eotaxin, G-CSF, M-CSF and IL-3) and inflammation (IL-6, IL-12, IFN-γ, CXCL10, CXCL1, TNF-α and VEGF) is comparison with that of WT foam cells.

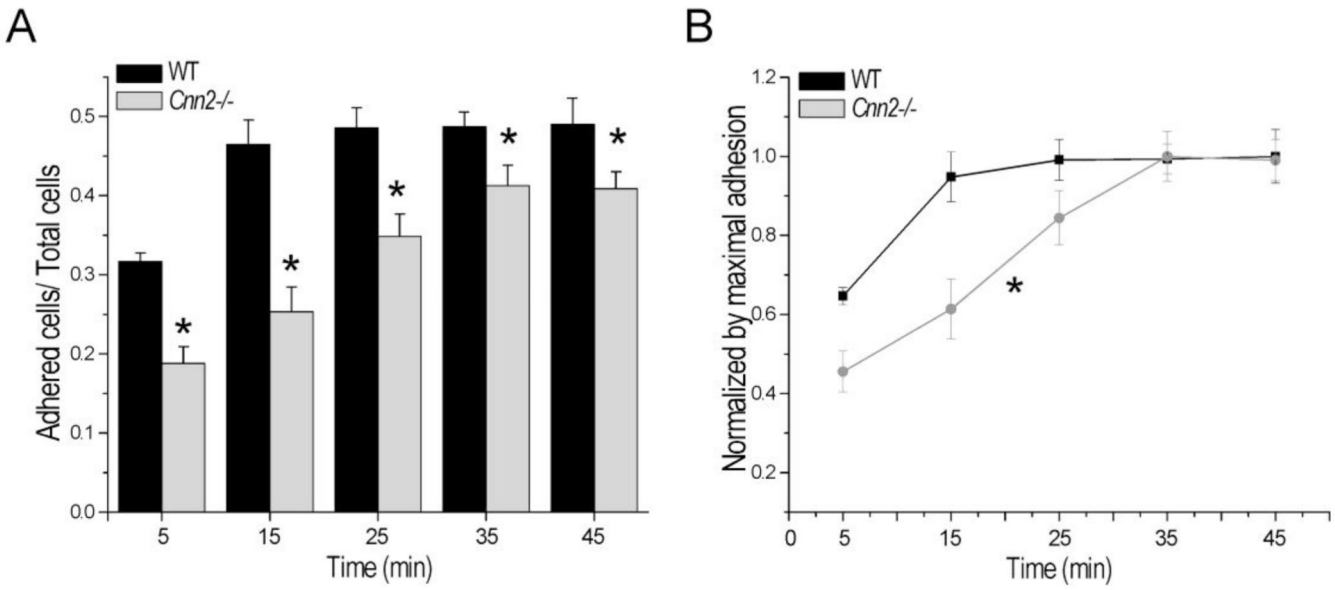

Figure 7. Decreased substrate adhesion of *Cnn2*$^{-/-}$ macrophages

Freshly isolated mouse peritoneal residential macrophages were studied for the velocity of substrate adhesion by quantification of the adherent cells at a series of time points. A. Normalized to the absorbance of the total seeded cells fixed in unwashed wells, the results showed that *Cnn2*$^{-/-}$ macrophages have a decreased substrate adhesion as compared with that of WT macrophages. B. Normalized to the maximum adherent cells of each group, the data further demonstrated that *Cnn2*$^{-/-}$ macrophages adhered to the culture substrate slower than that of WT macrophages, reaching the plateau of adhesion at 35 min vs. 15 min after seeding. *P<0.05 vs. WT group.

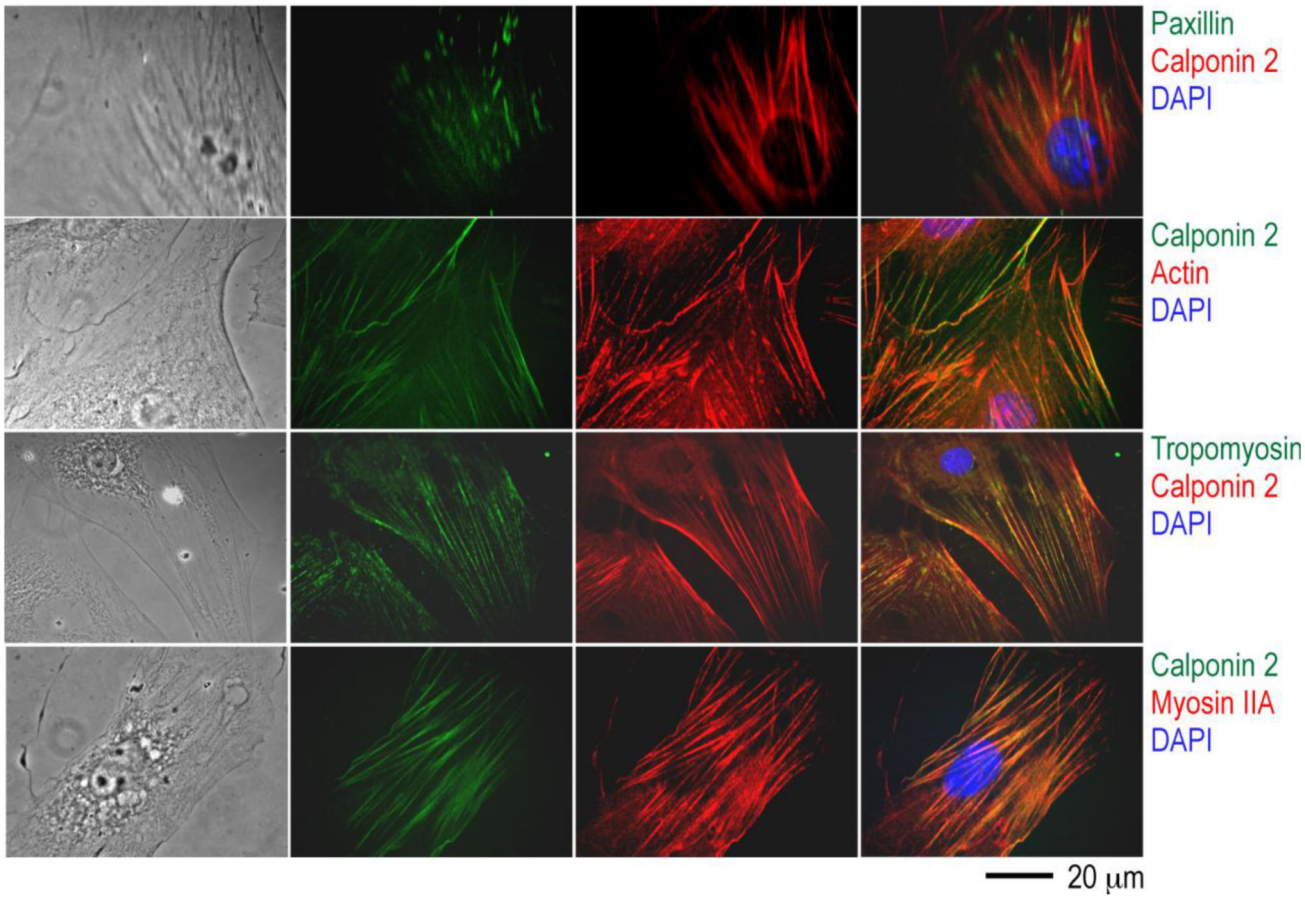

Figure 8. Association of calponin 2 with the actin-myosin cytoskeleton

Primary cultures of neonatal mouse skin fibroblasts on coverslips were examined. Confocal fluorescence microscopic images showed that calponin 2 co-localizes with tropomyosin-F-actin stress fibers (the distribution of tropomyosin detected using mAb CG3 is similar to that of F-actin stress fibers and co-localized with calponin 2) and myosin IIA, but not at the focal adhesion sites identified by anti-paxillin mAb 5H11 staining. Cell nucleus was stained with DAPI.

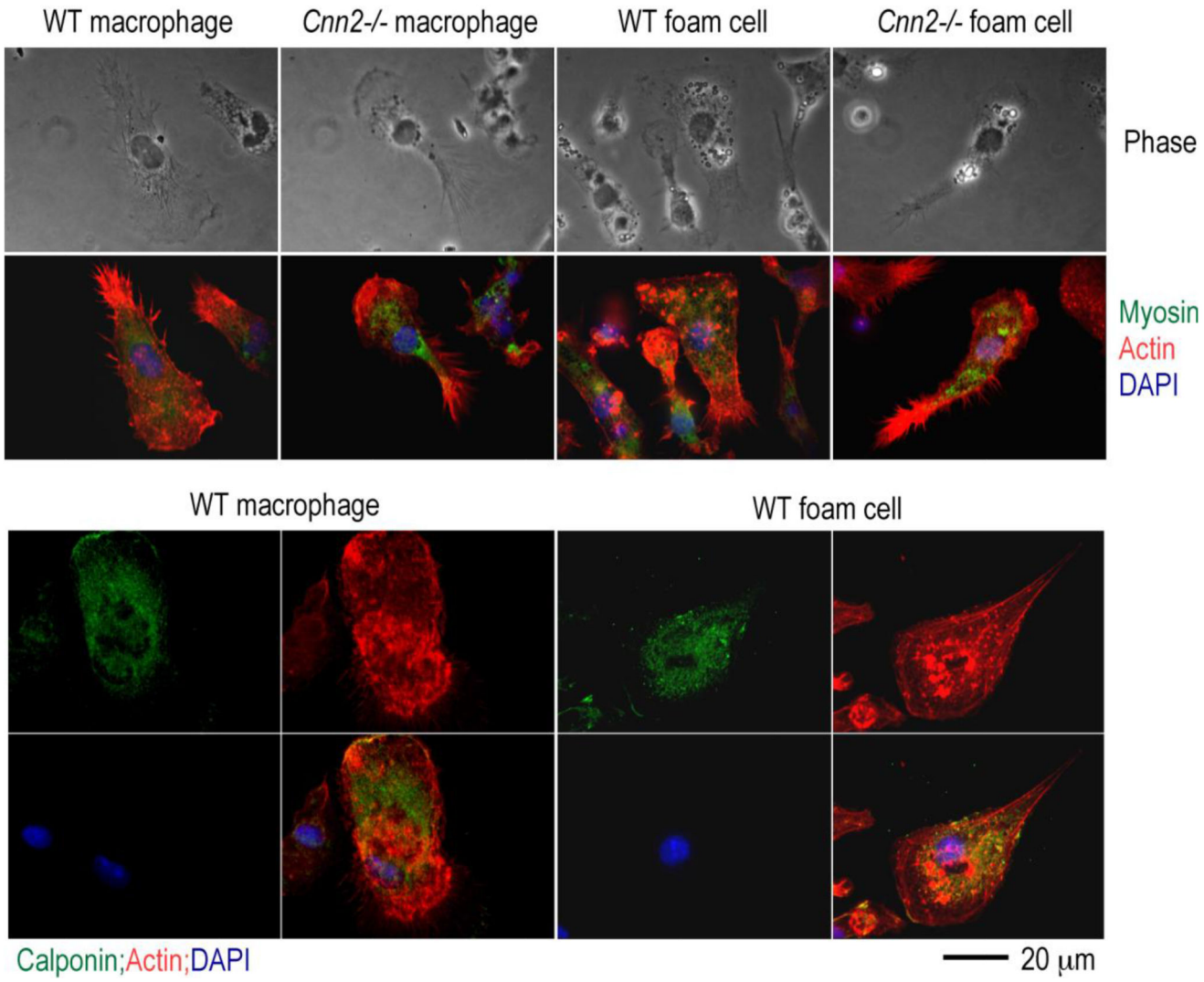

Figure 9. The actin-myosin cytoskeleton in WT and Cnn2$^{-/-}$ macrophages and foam cells

A. Confocal fluorescence microscopic images showed concentrated F-actin in the leading edge and the trailing tail of migrating macrophages, while myosin IIA mainly in the center of cell body and absent at the trailing tail. The distribution patterns of F-actin and myosin are similar in WT vs. Cnn2$^{-/-}$ macrophages and the foam cells. B. The cellular location of calponin 2 was investigated in WT macrophages and foam cells with F-actin as a reference. The results showed that calponin 2 is concentrated in the center of cell body and absent at the trailing tail, similar to that of myosin IIA. Cell nucleus was stained with DAPI.